Published in final edited form as:
Angew Chem Int Ed Engl. 2014 January 3; 53(1): 305–309. doi:10.1002/anie.201307849.

Organometallic Inhibitor for the Human Repair Enzyme 7,8-Dihydro-8-Oxoguanosine Triphosphatase

Manuel Streib,
Fachbereich Chemie, Philipps-Universität Marburg, Hans-Meerwein-Straße, 35043 Marburg (Germany)

Katja Kräling,
Fachbereich Chemie, Philipps-Universität Marburg, Hans-Meerwein-Straße, 35043 Marburg (Germany)

Kristin Richter,
Fachbereich Chemie, Philipps-Universität Marburg, Hans-Meerwein-Straße, 35043 Marburg (Germany)

Dr. Xiulan Xie,
Fachbereich Chemie, Philipps-Universität Marburg, Hans-Meerwein-Straße, 35043 Marburg (Germany)

Dr. Holger Steuber[†], and
LOEWE-Zentrum für Synthetische Mikrobiologie, Philipps-Universität Marburg, Hans-Meerwein-Straße, 35043 Marburg (Germany)

Prof., Dr. Eric Meggers
Fachbereich Chemie, Philipps-Universität Marburg, Hans-Meerwein-Straße, 35043 Marburg (Germany); College of Chemistry and Chemical Engineering, Xiamen University, Xiamen 361005 (People's Republic of China)

Holger Steuber: holger.steuber@bayer.com; Eric Meggers: meggers@chemie.uni-marburg.de

Keywords

Organometallic; ruthenium; enzyme inhibitor; 7,8-dihydro-8-oxoguanosine triphosphatase; protein crystal structure

A significant portion of all proteins encoded in the human genome bind or utilize purine-based nucleosides or nucleotides, such as ATP, GTP, NAD(P), FAD, PAPS, and coenzyme A.[1] These proteins, among which are important classes of enzymes such as kinases, ATPases, ligases, helicases, and chaperones, are involved in all types of cellular processes, are at the origin of many human diseases, and therefore constitute important targets for the design of small molecule drugs. Our group recently introduced a strategy for designing highly potent and selective ATP-mimetic inhibitors of protein kinases based on substitutionally inert transition metal complexes,[2,3] and we were wondering if –due to

[†]Current address: Bayer Pharma AG, Lead Discovery Berlin - Structural Biology, Müllerstrasse 178, 13353 Berlin (Germany)

certain common features of nucleotide binding sites[4]– inert transition metal complexes may constitute an attractive class of scaffolds for the development of inhibitors of other nucleotide binding proteins. We here now wish to report how we derived at a novel organoruthenium complex as the first low nanomolar and selective inhibitor of the human repair enzyme 7,8-dihydro-8-oxoguanosine triphosphatase (8-oxo-dGTPase, NUDT1, MTH1), an enzyme that hydrolyzes oxidized purine nucleoside triphosphates and thereby prevents their misincorporation into DNA.[5]

We started our study with the design of the organoruthenium half-sandwich complex **1**, containing a bidentate 8-(pyridin-2-yl)adenine ligand, an $\eta^{[5]}$-coordinated cyclopentadienyl moiety, and a CO ligand (Figure 1). Possessing a ruthenium-coordinated adenine nucleobase in combination with a molecular structure that is devised to mimic the overall shape of nucleotides, we envisioned organometallic **1** to serve as a probe for adenine nucleotide binding proteins. To verify this hypothesis, a probe-based technology using a biotinylated acyl phosphate derivative of ATP and ADP that can irreversibly react with conserved lysine residues in the pocket of ATP binding proteins was employed, thereby allowing to determine direct competition between probe and inhibitor binding within any biological sample.[6] Accordingly, when organometallic **1** was profiled at a concentration of 100 μM against more than 150 ATP-binding proteins within the lysate of HL60 cells,[7] **1** was identified to be a binder to a few cellular proteins, particularly the nuclear chaperone midasin and a homolog thereof,[8] a protein involved in the pyrimidine biosynthesis (CAD protein),[8] and the repair enzyme MTH1[5] (Figure 2). We chose MTH1 for further investigations since it plays an important role as a repair enzyme related to oxidative stress in cells and its inhibition might exhibit an interesting way to reduce cancer growth causing RAS-induced oxidative damage, leading to DNA double-strand-breaks, and provoking cells to enter premature senescence.[5] Furthermore, its co-crystal structure with bound 8-oxo-dGMP has been reported, thereby potentially facilitating the identification of important inhibitor-enzyme-interactions for further improvements of affinity.[10,11]

The concentration of **1** at which the activity of MTH1 is reduced to 50% (IC_{50} value) was determined with an HPLC assay to be a reasonable starting point with modest 151 μM (Figure 3). It is noteworthy that in addition to its affinity for 8-oxo-dGTP (K_m = 15.2 μM), MTH1 also binds and efficiently hydrolyses oxidized ATP derivatives (e.g. 8-oxo-dATP: K_m = 13.9 μM),[12] thus rationalizing why the adenine-containing nucleotide probe **1** possesses binding affinity to 8-oxo-dGTPase. Fortuitously, when we replaced the 8-(pyridin-2-yl)adenine ligand of **1** against a cyclometalated 4-amino-6-(pyridin-2-yl)quinazoline, obtaining complex **2**, the IC_{50} value was improved by more than two orders of magnitude to 1.1 μM. A subsequent structure-activity relationship with this metallo-quinazoline lead structure by derivatizing the cyclopentadienyl moiety afforded complex **3**, displaying a further decreased IC_{50} value of 38 nM (see Supporting Information for additional derivatives). Finally, the introduction of a methyl group at position 2 of the quinazoline moiety provided a single digit nanomolar inhibitor for MTH1 (IC_{50} = 6 nM for complex **4**). Compared with the initial probe **1**, the organometallic inhibitor **4** displays an improved affinity for MTH1 by a factor of around 26,000.

To understand the binding of the organometallic **4** to MTH1, we co-crystallized racemic **4** with MTH1 and solved the structure to a resolution of 2.70 Å (Table 1).[13] Figure 4 shows the overall structure. As a member of the Nudix hydrolases superfamily,[14] MTH1 exhibits the typical Nudix fold with an arrangement of a mixed β-sheet surrounded by two α-helixes, which together with several loops creates the active site. As expected, the organometallic **4** occupies the 8-oxo-dGTP binding site and the electron density distribution, especially of the phenolic ester moiety, allows a clear assignment of the *S*-configuration at the stereogenic metal center.[15] As visualized by the semi-transparent surface view in Figure 4, complex **4** is tightly surrounded by residues from the α-helices, β-sheets, and loops to provide an interaction surface of approximately 501 $Å^{2}$.[16] The quinazoline moiety forms several hydrogen bonds, one between the exocyclic NH_2 group and Asp119, one between the endocyclic N3 and Asp120, in addition to the endocyclic N1 being in hydrogen bonding distance to the backbone NH of Gly34 and the amide side chain of Asn33 (Figure 5a). Further polar contacts at a larger distance can be identified between the ester carbonyl group of **4** and Lys23, and between a methoxy group of **4** and the backbone NH group of Lys38. The inhibitor is in van-der-Waals contact with multiple side chains such as highlighted in Figure 5b. Especially intriguing are the number of aromatic side chains stacking face-to-face (Trp117 and Phe27) or edge-to-face (Trp123, Phe72, Tyr7) to the inhibitor. In order to compare the binding of (*S*)-**4** with 8-oxo-dGMP (PDB ID 3ZR0[10]), both co-crystal structures were superimposed. As displayed in Figure 5c, the pyridylquinazoline moiety of (*S*)-**4** co-locates roughly with the guanine nucleobase of 8-oxo-dGMP, the ruthenium center aligns with the ribose unit, whereas the 2,6-dimethoxyphenylester fills the space occupied by the phosphate of 8-oxo-dGMP. Although the position of the heteroaromatic quinazoline moiety is somewhat shifted and tilted compared to the purine nucleobase of 8-oxo-dGMP, the same key residues are involved in hydrogen bonding to both ligands, which is possible since the guanine base of 8-oxo-dGMP apparently adopts the enol tautomeric form.[10]

Overall, the high affinity of (*S*)-**4** to MTH1 can be rationalized by a combination of several hydrogen bonding interactions, a large number of close van-der-Waals contacts, and a shape match between the nucleotide binding site and the organometallic inhibitor. The limited conformational flexibility of **4** does not only provide an entropic advantage, which is reflected in the high binding affinity to MTH1, but also contributes to an impressive specificity. In fact, organometallic **4** does not show any notable protein kinase binding at a concentration of 1 μM as verified in an active-site-directed competition binding assay against a panel of 457 kinases (see Supporting Information).[17,18] Furthermore, profiling of **4** at 10 μM against 191 protein ATP binding sites confirmed the high selectivity of **4** with only MTH1 and deoxycytidine kinase competing by more than 50% with the reactive acyl phosphate ATP probe (see Supporting Information).

In summary, we here presented the discovery of the first small molecule inhibitor of the repair enzyme 8-oxo-dGTPase (MTH1), which is not a canonical small organic molecule but rather an unconventional cyclometalated ruthenium half sandwich complex. The low nanomolar organometallic inhibitor displays an astonishing specificity as verified in an extended panel of protein kinases and other ATP binding proteins. These results reinforce conclusions drawn from our previous work on metal-based inhibitors of protein kinases,

namely that inert metal complexes constitute excellent scaffolds for obtaining highly selective molecular probes, which we attribute to the limited flexibility of the globular metal complexes.[19] Furthermore, this work provides a blueprint for the discovery and development of organometallic inhibitors of other purine nucleotide binding proteins by using ruthenium coordinated adenine and quinazoline derivatives with different coordination spheres. Finally, the novel organometallic MTH1 inhibitor **4** will be employed as a tool for a closer investigation of the biological function of MTH1 and its merit to serve as a target for anticancer therapy.

Supplementary Material

Refer to Web version on PubMed Central for supplementary material.

Acknowledgments

This work was funded by the German Research Foundation (ME1805-9/1) and the US National Institutes of Health (CA114046). A generous gift of the MTH1 expression vector from Pär Nordlund (Structural Genomics Consortium) is gratefully acknowledged. The authors thank the staff of the Bessy MX department for providing beamtime, equipment and support for data collection. We thank the Helmholtz-Zentrum Berlin (HZB) for synchrotron travel grants.

References

1. The human purinome: Haystead TAJ. Curr Top Med Chem. 2006; 6:1117–1127. [PubMed: 16842150] ; Knapp M, Bellamacina C, Murray JM, Bussiere DE. Curr Top Med Chem. 2006; 6:1129–1159. [PubMed: 16842151] ; Murray JM, Bussiere DE. Methods Mol Biol. 2009; 575:47–92. [PubMed: 19727611]
2. For applications of metal-containing compounds in the life sciences, see: Fish RH, Jaouen G. Organometallics. 2003; 22:2166–2177.; Jaouen G. Bioorganometallics. Wiley-VCHWeinheim2005; Hannon MJ. Chem Soc Rev. 2007; 36:280–295. [PubMed: 17264930] ; Alberto R. J Organomet Chem. 2007; 692:1179–1186.; Zeglis BM, Pierre VC, Barton JK. Chem Commun. 2007:4565–4579.; Hambley TW. Science. 2007; 318:1392–1393. [PubMed: 18048674] ; Hambley TW. Dalton Trans. 2007:4929–4937. [PubMed: 17992277] ; Levina A, Mitra A, Lay PA. Metallomics. 2009; 1:458–470. [PubMed: 21305154] ; Keene FR, Smith JA, Collins JG. Coord Chem Rev. 2009; 253:2021–2035.; Haas KL, Franz KJ. Chem Rev. 2009; 109:4921–4960. [PubMed: 19715312] ; Schatzschneider U. Eur J Inorg Chem. 2010:1451–1467.; Che CM, Siu FM. Curr Opin Chem Biol. 2010; 14:255–261. [PubMed: 20018553] ; Gasser G, Ott I, Metzler-Nolte N. J Med Chem. 2011; 54:3–25. [PubMed: 21077686] ; Hillard EA, Jaouen G. Organometallics. 2011; 30:20–27.; Meggers E. Angew Chem Int Ed. 2011; 50:2442–2448.; Rouffet M, Cohen SM. Dalton Trans. 2011; 40:3445–3454. [PubMed: 21290034] ; Salassa L. Eur J Inorg Chem. 2011:4931–4947.; Bergamo A, Sava G. Dalton Trans. 2011; 40:7817–7823. [PubMed: 21629963] ; Patra M, Gasser G. ChemBioChem. 2012; 13:1232–1252. [PubMed: 22619182] ; Ball ZT. Acc Chem Res. 2013; 46:560–570. [PubMed: 23210518] ; Hartinger CG, Metzler-Nolte N, Dyson PJ. Organometallics. 2012; 31:5677–5685.; Sasmal PK, Streu CN, Meggers E. Chem Commun. 2013; 49:1581–1587.; Barry NPE, Sadler PJ. Chem Commun. 2013; 49:5106–5131.; Kilah NL, Meggers E. Aust J Chem. 2012; 65:1325–1332.; Kilpin KJ, Dyson PJ. Chem Sci. 2013; 4:1410–1419.
3. Meggers E, Atilla-Gokcumen GE, Bregman H, Maksimoska J, Mulcahy SP, Pagano N, Williams DS. Synlett. 2007; 8:1177–1189.
4. Chène P. Nat Rev Drug Disc. 2002; 1:665–673.
5. Nakabeppu Y, Oka S, Sheng Z, Tsuchimoto D, Sakumi K. Mutat Res. 2010; 703:51–58. [PubMed: 20542142]
6. a.) Patricelli MP, Szardenings AK, Liyanage M, Nomanbhoy TK, Wu M, Weissig H, Aban A, Chun D, Tanner S, Kozarich JW. Biochemistry. 2007; 46:350–358. [PubMed: 17209545] b.) Patricelli MP, Nomanbhoy TK, Wu J, Brown H, Zhou D, Zhang J, Jagannathan S, Aban A, Okerberg E,

Herring C, Nordin B, Weissig H, Yang Q, Lee JD, Gray NS, Kozarich JW. Chem Biol. 2011; 18:699–710. [PubMed: 21700206]

7. Complex **4** is stable in DMSO-d_6/D_2O (9:1; 5 mM) at room temperature in the presence of an equimolar amount of 2-mercaptoethanol for at least seven days as has been verified by ^{1}H-NMR.
8. Garbarino JE, Gibbons IR. BMC Genomics. 2002; 3:18. [PubMed: 12102729]
9. Kim H, Kelly RE, Evans DR. J Biol Chem. 1992; 267:7177–7184. [PubMed: 1348059]
10. Svensson LM, Jemth AS, Desroses M, Loseva O, Helleday T, Högbom M, Stenmark P. FEBS Lett. 2011; 585:2617–2621. [PubMed: 21787772]
11. For a solution structure of MTH1, see: Mishima M, Sakai Y, Itoh N, Kamiya H, Furuichi M, Takahashi M, Yamagata Y, Iwai S, Nakabeppu Y, Shirakawa M. J Biol Chem. 2004; 279:33806–33815. [PubMed: 15133035]
12. a.) Fujikawa K, Kamiya H, Yakushiji H, Fujii Y, Nakabeppu Y, Kasai H. J Biol Chem. 1999; 274:18201–18205. [PubMed: 10373420] b.) Fujikawa K, Kamiya H, Yakushiji H, Nakabeppu Y, Kasai H. Nucl Acids Res. 2001; 29:449–454. [PubMed: 11139615]
13. For co-crystal structures of organometallic half-sandwich and sandwich compounds bound non-covalently to proteins, see: Debreczeni JÉ, Bullock AN, Atilla GE, Williams DS, Bregman H, Knapp S, Meggers E. Angew Chem Int Ed. 2006; 45:1580–1585.; Pagano N, Maksimoska J, Bregman H, Williams DS, Webster RD, Xue F, Meggers E. Org Biomol Chem. 2007; 5:1218–1227. [PubMed: 17406720] ; Maksimoska J, Feng L, Harms K, Yi C, Kissil J, Marmorstein R, Meggers E. J Am Chem Soc. 2008; 130:15764–15765. [PubMed: 18973295] ; Atilla-Gokcumen GE, Pagano N, Streu C, Maksimoska J, Filippakopoulos P, Knapp S, Meggers E. Chembiochem. 2008; 9:2933–2936. [PubMed: 19035373] ; Xie P, Williams DS, Atilla-Gokcumen GE, Milk L, Xiao M, Smalley KS, Herlyn M, Meggers E, Marmorstein R. ACS Chem Biol. 2008; 3:305–316. [PubMed: 18484710] ; Xie P, Streu C, Qin J, Bregman H, Pagano N, Meggers E, Marmorstein R. Biochemistry. 2009; 48:5187–5198. [PubMed: 19371126] ; Bullock AN, Russo S, Amos A, Pagano N, Bregman H, Debreczeni JÉ, Lee WH, von Delft F, Meggers E, Knapp S. PLoS One. 2009; 4:e7112. [PubMed: 19841674] ; Atilla-Gokcumen GE, Di Constanzo L, Meggers E. J Biol Inorg Chem. 2011; 16:45–50. [PubMed: 20821241] ; Blanck S, Geisselbrecht Y, Kräling K, Middel S, Mietke T, Harms K, Essen LO, Meggers E. Dalton Trans. 2012; 41:9337–9348. [PubMed: 22733119] ; Salmon AJ, Williams ML, Hofmann A, Poulsen SA. Chem Commun. 2012; 48:2328–2330.; Can D, Spingler B, Schmutz P, Mendes F, Raposinho P, Fernandes C, Carta F, Innocenti A, Santos I, Supuran CT, Alberto R. Angew Chem Int Ed. 2012; 51:3354–3357.
14. Mildvan AS, Xia Z, Azurmendi HF, Saraswat V, Legler PM, Massiah MA, Gabelli SB, Bianchet MA, Kang LW, Amzel LM. Arch Biochem Biophys. 2005; 433:129–143. [PubMed: 15581572]
15. The absolute configuration at the ruthenium center was assigned according to the priority order of the ligands as Cp > N > CO > C
16. The interaction surface was calculated using PISA (PDBe PISA v1.47) as accessible via http://pdbe.org/pisa. The given value is the average of the interaction interfaces obtained from both complexes in the asymmetric unit.
17. a.) Fabian MA, Biggs WH III, Treiber DK, Atteridge CE, Azimioara MD, Benedetti MG, Carter TA, Ciceri P, Edeen PT, Floyd M, Ford JM, Galvin M, Gerlach JL, Grotzfeld RM, Herrgard S, Insko DE, Insko MA, Lai AG, Lélias JM, Mehta SA, Milanov ZV, Velasco AM, Wodicka LM, Patel HK, Zarrinkar PP, Lockhardt DJ. Nat Biotechnol. 2005; 23:329–336. [PubMed: 15711537] b.) Karaman MW, Herrgard S, Treiber DK, Gallant P, Atteridge CE, Campbell BT, Chan KW, Ciceri P, Davis MI, Edeen PT, Faraoni R, Floyd M, Hunt JP, Lockhardt DJ, Milanov ZV, Morrison MJ, Pallares G, Patel HK, Pritchard S, Wodicka LM, Zarrinkar PP. Nat Biotechnol. 2008; 26:127–132. [PubMed: 18183025]
18. This might at least partly result from the additional C2-methyl substituent which sterically disturbs the hydrogen bonding between inhibitor and the backbone of the hinge region of protein kinases. In contrast, in the case of MTH1 even an ethyl substituent is tolerated without significant loss of affinity (see Supporting Information).
19. a.) Feng L, Geisselbrecht Y, Blanck S, Wilbuer A, Atilla-Gokcumen GE, Filippakopoulos P, Kräling K, Celik MA, Harms K, Maksimoska J, Marmorstein R, Frenking G, Knapp S, Essen LO, Meggers E. J Am Chem Soc. 2011; 133:5976–5986. [PubMed: 21446733] b.) Blanck S,

Maksimoska J, Baumeister J, Harms K, Marmorstein R, Meggers E. Angew Chem Int Ed. 2012; 51:5244–5246.

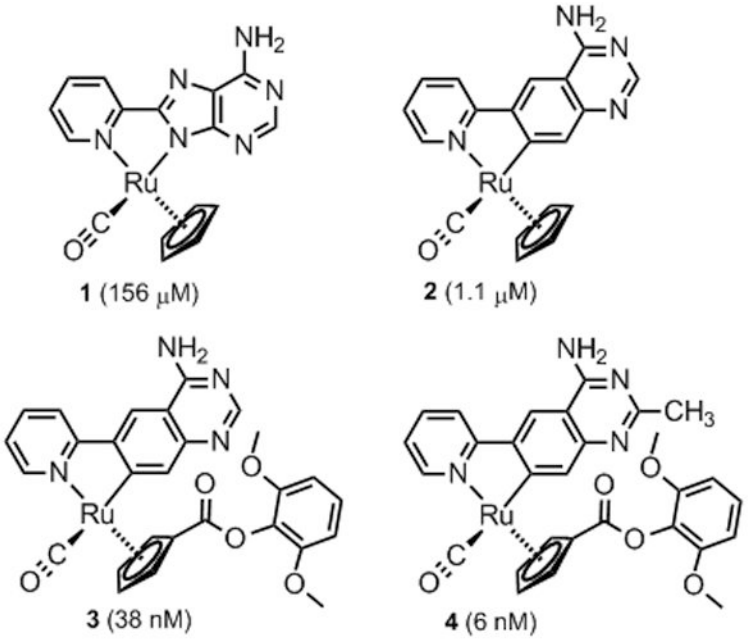

Figure 1.

Organometallics investigated and developed as inhibitors for human 8-oxo-dGTPase (MTH1, NUDT1). Determined IC_{50} values are given in brackets. All complexes were synthesized and used as racemates.

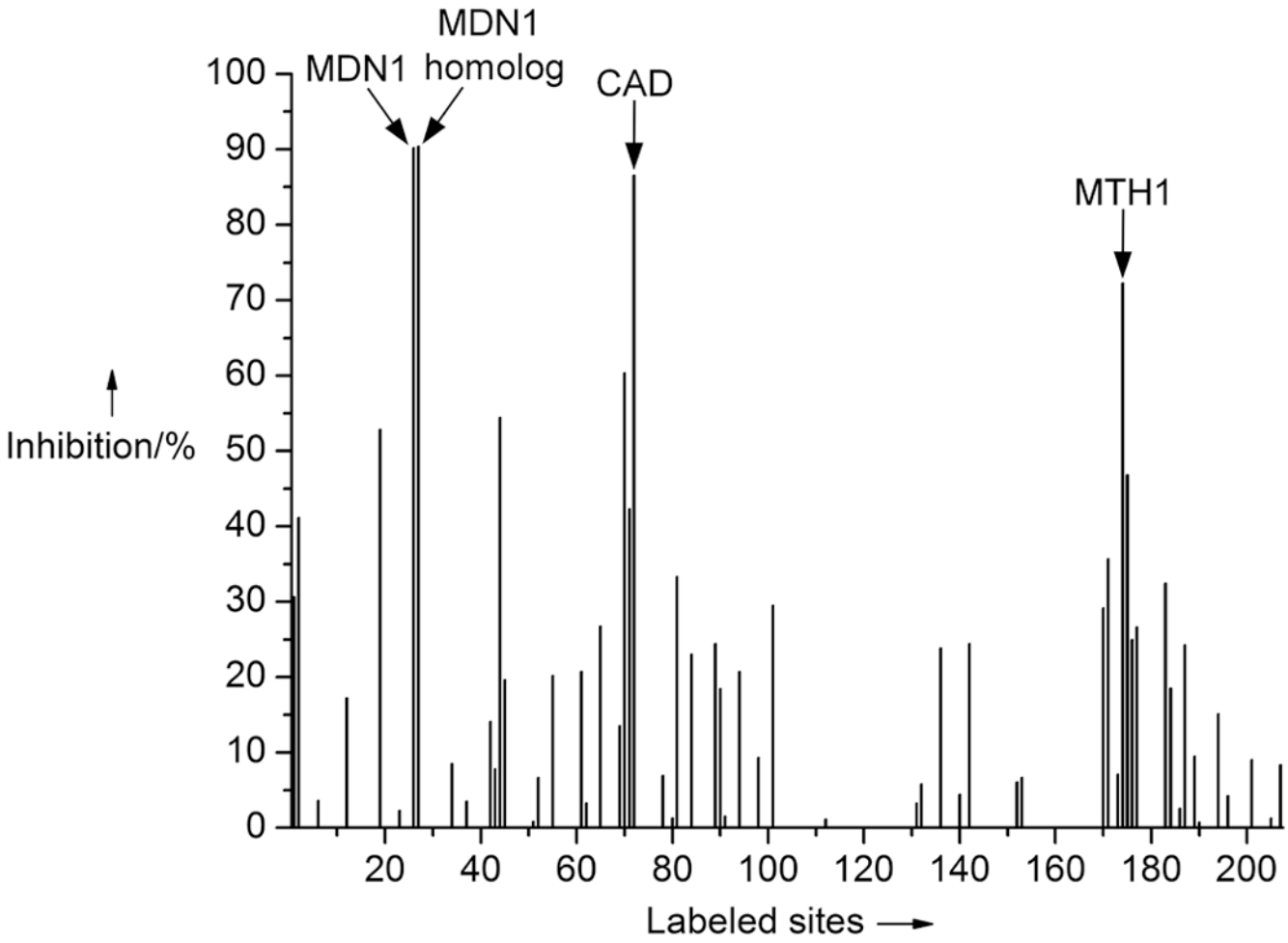

Figure 2.

Profiling of complex **1** (100 μM) against ATP binding proteins within the cell lysate of HL60 cells with probe technology (KiNativ™, ActivX Biosciences, La Jolla, CA, USA) using a biotinylated acyl phosphate derivative of ATP and ADP. Shown is the inhibition of probe binding by complex **1** to 207 confirmed sites of 153 ATP binding proteins. Main hits: Midasin (MDN1, 90% inh.), a midasin homolog (90% inh.), CAD protein (87% inh.), and 8-oxo-dGTPase (MTH1/NUDT1, 72% inh.). See Supporting Information for more details.

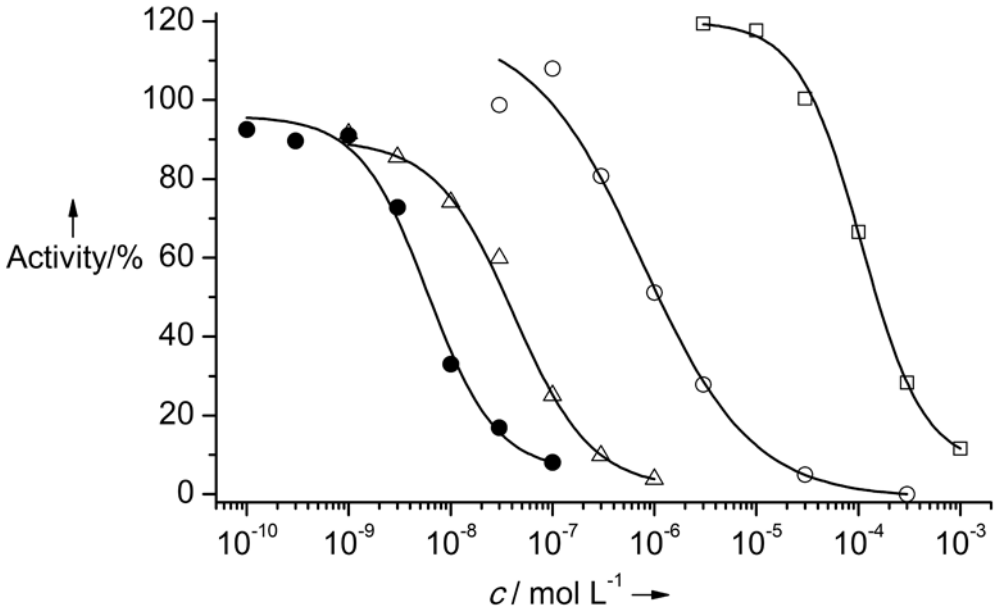

Figure 3.

Inhibition curves of complexes **1**-**4** against MTH1: **1** = empty squares, **2** = empty circles, **3** = empty triangles, **4** = filled circles. Assay conditions: Organometallics **1**-**4** were preincubated with purified MTH1 (10 nM) for 30 min. After addition of 8-oxo-dGTP (25 μM) and incubation for 10 min at 37 °C under shaking, the reaction was quenched and analyzed *via* HPLC for quantification of the starting material 8-oxo-dGTP and the product 8-oxo-dGMP.

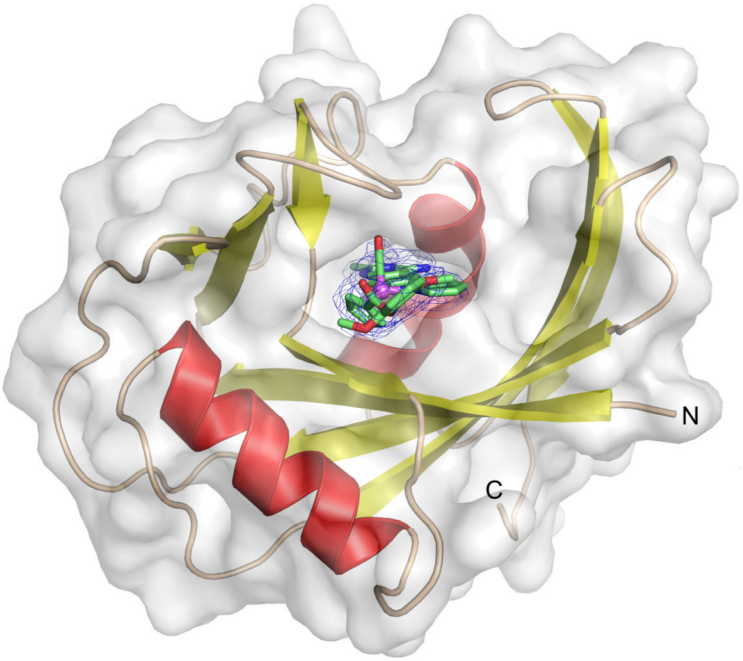

Figure 4.

Co-crystal structure of MTH1 (chain A, semintransparent surface view) with organoruthenium compound (*S*)-**4** bound to the nucleotide binding site. The absolute configuration of the inhibitor was elucidated from its electron-density (shown as blue mesh). The SIGMAA-weighted $2F_{obs} - F_{calc}$ difference electron density map of the inhibitor was contoured at 1 σ.

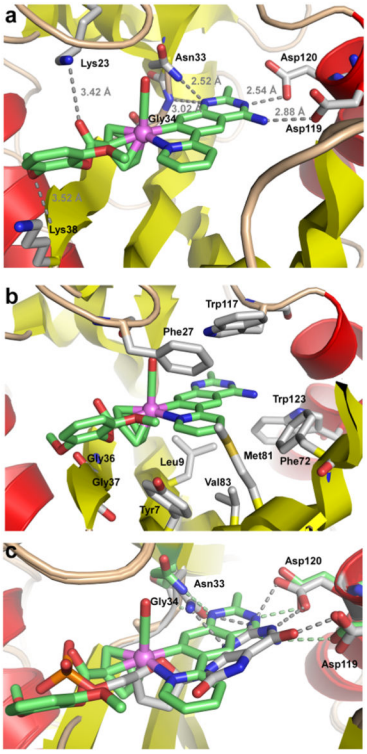

Figure 5.

Interactions of (*S*)-**4** with the active site residues of MTH1 and superimposed co-crystal structures of (*S*)-**4** (green) and 8-oxo-dGMP (grey) with MTH1 (pdb: 3ZR0). Alignment was accomplished with PyMOL Molecular Graphics System, Version 0.99rc6, Schrödinger, LLC.

Table 1

Crystallographic data and refinement statistics for **4**/MTH1 (PDB entry 3WHW).

Data collection and Processing	
No. of crystals used	1
Wavelength [Å]	0.91841
Space group	P 21 21 21
Unit cell parameters	
a, b, c [Å]	59.76, 67.65, 79.54
α,β,γ [°]	90, 90, 90
Matthews coefficient [$Å^3$/Da]	2.21
Solvent content [%]	44.2
Diffraction data	
Resolution range [Å]	25.0 – 2.70 (2.90-2.70)
Unique reflections	9264 (1737)
$R(I)_{sym}$ [%]	16.0 (63.3)
Completeness [%]	99.6 (99.0)
Redundancy	5.8 (5.7)
I/σ(I)	10.62 (3.0)
Refinement	
Resolution range [Å]	25.0 – 2.70
Reflections used in refinement (work/free)	8800 / 464
Final R values for all reflections (work/free) [%]	21.5 / 26.6
Protein residues	308
Inhibitor atoms	78
Water molecules	34
Sulfate ions	7
RMSDs	
Bonds [Å]	0.0085
Angles [°]	1.280
Ramachandran plot	
Residues in most favoured regions [%]	89.6
Residues in additional allowed regions [%]	10.4
Residues in generously allowed regions [%]	-
Mean B factor [$Å^2$]	
Protein	51.9
Inhibitor	58.9
Water molecules	33.4
Sulfate ions	99.8